A new method for eigenproblems with circular boundaries

C.T. Chen[1], I.L. Chen[2], J.T. Chen[1]

[1]Department of Harbor and River Engineering, National Taiwan Ocean University

[2]Department of Naval Architecture, National Kaohsiung Marine University

Abstract

In this paper, the eigenproblems with circular boundaries are studied by using null-field integral equations in conjunction with degenerate kernels and Fourier series. Direct-searching scheme is employed to detect the eigenvalues by using singular value decomposition (SVD) technique. It is analytically verified that an inner circle results in the spurious eigenvalue and it appears in the numerical experiment. Also, the spurious eigenequation due to the inner circle is examined. Several examples are demonstrated to see the validity of the present formulation.

Keywords: null-field integral equation, singular value decomposition, degenerate kernel, Fourier series, eigenproblem.

Introduction

Boundary element method (BEM) and finite element method (FEM) have been recognized as alternatives for solving eigenproblems. Although FEM is a popular method for solving eigenproblems, it needs a lot of time to generate the mesh. In this aspect, BEM is an efficient alternative from the viewpoint of mesh reduction. No mesh is our final goal. For multiply-connected domain problems, spurious eigensolution in the BEM [1-3] and MFS [4-6] has been noticed until the recent years. To solve multiply-connected eigenproblems, Lin [7] employed the transformation technique of cylindrical wave functions to satisfy the boundary condition with seven holes. Nagaya and Poltorak [8] used both the Fourier expansion collocation method and point-matching approach to find the eigenvalues of elliptical or polygonal outer boundary with eccentric inner boundaries. Chen *et al*. [1-3] used the BEM to determine the eigenvalue and eigenmode for the multiply-connected eigenproblems. The spurious eigensolution was found and filtered out by using the SVD updating technique and the Burton & Miller method.

In this paper, the boundary integral equation method (BIEM) is utilized to solve the eigenproblems with circular boundaries. To fully utilize the geometry of circular boundary, Fourier series for boundary densities and degenerate kernel for fundamental solutions are incorporated into the null-field integral equation. Direct-searching scheme is adopted to detect the eigenvalue by using the SVD technique. Mode shape can be simultaneously determined from the right unitary vectors of zero singular value. The results will be compared with those of FEM and BEM.

Problem Statement and Integral Formulation

Consider the eigenproblem with a circular domain containing N randomly distributed circular holes centered at position vector $\underset{\sim}{c}_j$ (j =1, 2, ..., N) as shown in Fig. 1. Let a_j and B_j denote the radius and boundary of the *jth* circular hole.

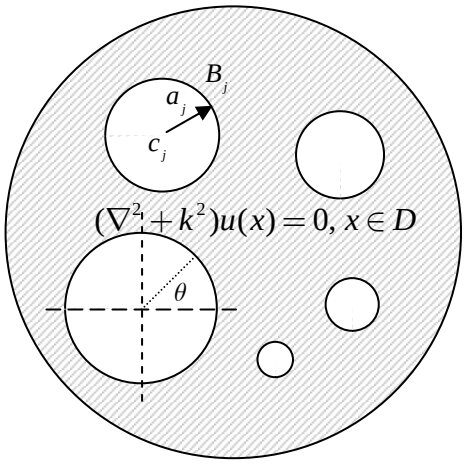

FIGURE 1. Problem statement

By employing the Fourier series expansions to approximate the potential u and its normal flux t on the boundary, we have

$$u(\underset{\sim}{s}) = a_{0j} + \sum_{n=1}^{\infty}(a_{nj}\cos n\theta_j + b_{nj}\sin n\theta_j), \underset{\sim}{s}\in B_j \quad (1)$$

$$t(\underset{\sim}{s}) = p_{0j} + \sum_{n=1}^{\infty}(p_{nj}\cos n\theta_j + q_{nj}\sin n\theta_j), \underset{\sim}{s}\in B_j \quad (2)$$

where a_{0j}, a_{nj}, b_{nj}, p_{0j}, p_{nj} and q_{nj} are the Fourier coefficients and θ_j is the polar angle centered at c_j. Based on the boundary integral formulation of the domain point for the eigenproblem, we have

$$2\pi u(\underset{\sim}{x}) = \int_B T(\underset{\sim}{s},\underset{\sim}{x})u(\underset{\sim}{s})dB(\underset{\sim}{s}) - \int_B U(\underset{\sim}{s},\underset{\sim}{x})t(\underset{\sim}{s})dB(\underset{\sim}{s}), \underset{\sim}{x}\in D \quad (3)$$

where $\underset{\sim}{s}$ and $\underset{\sim}{x}$ are the source and field points, respectively, D is the domain of interest, B is the boundary and $U(\underset{\sim}{x},\underset{\sim}{s})$ is the fundamental solution which satisfies

$$(\nabla^2+k^2)U(\underset{\sim}{x},\underset{\sim}{s}) = 2\pi\delta(\underset{\sim}{x}-\underset{\sim}{s}) \quad (4)$$

in which, $\delta(\underset{\sim}{x}-\underset{\sim}{s})$ denotes the Dirac-delta function. The $T(\underset{\sim}{s},\underset{\sim}{x})$ kernel, is defined by

$$T(\underset{\sim}{s},\underset{\sim}{x}) = \frac{\partial U(\underset{\sim}{s},\underset{\sim}{x})}{\partial n_{\underset{\sim}{s}}} \quad (5)$$

where $n_{\underset{\sim}{s}}$ denotes the outward normal vector at the source point *s*. By collocating $\underset{\sim}{x}$ outside the domain ($\underset{\sim}{x}\in D^e$), we obtain the null-field integral equation as shown below

$$0 = \int_B T(\underset{\sim}{s},\underset{\sim}{x})u(\underset{\sim}{s})dB(\underset{\sim}{s}) - \int_B U(\underset{\sim}{s},\underset{\sim}{x})t(\underset{\sim}{s})dB(\underset{\sim}{s}), \underset{\sim}{x}\in D^e. \quad (6)$$

Based on the separable property, the fundamental function can be expanded into degenerate kernel form as shown below

$$U(s,x) = \begin{cases} U^I(\underset{\sim}{s},\underset{\sim}{x}) = \dfrac{-\pi i}{2}\displaystyle\sum_{m=0}^{\infty}\varepsilon_m J_m(k|\underset{\sim}{x}-\underset{\sim}{c}_j|) H_m^{(1)}(k|\underset{\sim}{s}-\underset{\sim}{c}_j|)\cos(m\alpha), \\ \qquad |\underset{\sim}{s}-\underset{\sim}{c}|>|\underset{\sim}{x}-\underset{\sim}{c}| \\ U^E(\underset{\sim}{s},\underset{\sim}{x}) = \dfrac{-\pi i}{2}\displaystyle\sum_{m=0}^{\infty}\varepsilon_m H_m^{(1)}(k|\underset{\sim}{x}-\underset{\sim}{c}_j|) J_m(k|\underset{\sim}{s}-\underset{\sim}{c}_j|)\cos(m\alpha), \\ \qquad |\underset{\sim}{x}-\underset{\sim}{c}|>|\underset{\sim}{s}-\underset{\sim}{c}| \end{cases} \quad (7)$$

where $i^2=-1$, α is the angle between $\underset{\sim}{s}-\underset{\sim}{c}_j$ and $\underset{\sim}{x}-\underset{\sim}{c}_j$, the superscripts I and E denote the interior and exterior cases, respectively, and

$$\varepsilon_m = \begin{cases} 1, & m=0, \\ 2, & m\neq 0, \end{cases} \quad (8)$$

After taking the normal derivative with respect to *U* kernel, the $T(\underset{\sim}{s},\underset{\sim}{x})$ kernel can be derived as

$$T(s,x) = \begin{cases} T^I(\underset{\sim}{s},\underset{\sim}{x}) = \dfrac{-\pi i}{2}\displaystyle\sum_{m=0}^{\infty}\varepsilon_m J_m(k|\underset{\sim}{x}-\underset{\sim}{c}_j|) \{\dfrac{\partial H_m^{(1)}(k|\underset{\sim}{s}-\underset{\sim}{c}|)}{\partial n_{\underset{\sim}{s}}}\cos(m\alpha) + H_m^{(1)}(k|\underset{\sim}{s}-\underset{\sim}{c}|)\dfrac{\partial\cos(m\alpha)}{\partial n_{\underset{\sim}{s}}}\}, \\ \qquad |\underset{\sim}{s}-\underset{\sim}{c}|>|\underset{\sim}{x}-\underset{\sim}{c}| \\ T^E(\underset{\sim}{s},\underset{\sim}{x}) = \dfrac{-\pi i}{2}\displaystyle\sum_{m=0}^{\infty}\varepsilon_m H_m^{(1)}(k|\underset{\sim}{x}-\underset{\sim}{c}_j|) \{\dfrac{\partial J_m(k|\underset{\sim}{s}-\underset{\sim}{c}|)}{\partial n_{\underset{\sim}{s}}}\cos(m\alpha) + J_m(k|\underset{\sim}{s}-\underset{\sim}{c}|)\dfrac{\partial\cos(m\alpha)}{\partial n_{\underset{\sim}{s}}}\}, \\ \qquad |\underset{\sim}{x}-\underset{\sim}{c}|>|\underset{\sim}{s}-\underset{\sim}{c}| \end{cases} \quad (9)$$

In the real computation, only finite M terms are used in the summation of Eqs. (1) and (2).

Linear Algebraic Equation

By collocating the null-field point on the kth circular boundary for Eq. (6), we have

$$0=\sum_{j=1}^{N_c}\int_{B_j} T(\underset{\sim}{s},\underset{\sim}{x}_k)u(\underset{\sim}{s})dB(\underset{\sim}{s}) - \sum_{j=1}^{N_c}\int_{B_j} U(\underset{\sim}{s},\underset{\sim}{x}_k)t(\underset{\sim}{s})dB(\underset{\sim}{s}),\ \underset{\sim}{x}_k\in D^e \tag{10}$$

where N_c is the number of circles. It is noted that the path is anticlockwise for the outer circle. Otherwise, it is clockwise. For the B_j integral of the circular boundary, the kernels of $U(\underset{\sim}{s},\underset{\sim}{x})$ and $T(\underset{\sim}{s},\underset{\sim}{x})$ are respectively expressed in terms of degenerate kernels of Eqs. (7) and (8), and $u(\underset{\sim}{s})$ and $t(\underset{\sim}{s})$ are substituted by using the Fourier series of Eqs. (1) and (2), respectively. In the B_j integration, we set the origin of the observer system to collocate at the center c_j to fully utilize the degenerate kernel and Fourier series. By collocating the null-field point near B_k, Fig. 2 (a) shows the collocation point and boundary contour. A linear algebraic system is obtained

$$[U]\{x\}=[T]\{y\} \tag{11}$$

where $[U]$ and $[T]$ are the influence matrices, $\{x\}$ and $\{y\}$ denote the vectors $t(\underset{\sim}{s})$ and $u(\underset{\sim}{s})$ of Fourier coefficient, respectively. For simplicity, the Dirichlet case of $u(s)=0$ is considered. We can obtain nonlinear eigenequation.

$$[U]\{x\}=0 \tag{12}$$

By employing the direct-searching scheme, SVD technique can obtain the eigenvalues and boundary modes at the same time. After obtaining the eigenvalues and unknown Fourier coefficients, the origin of observer system is set to c_j in the B_j integration as shown in Fig. 2 (b) to obtain the interior potential by employing Eq. (3). The boundary integrals on the circle are listed in the Appendix. The flow chart of the present method is shown in Fig. 2 (c).

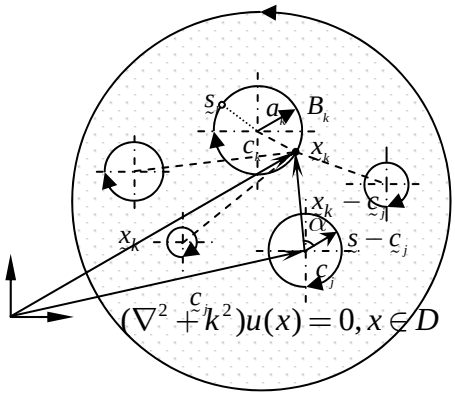

FIGURE 2 (a) Null-field integral equation

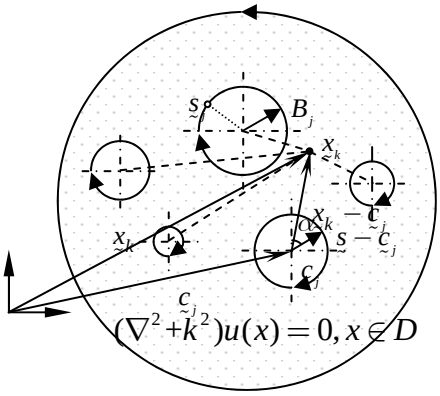

FIGURE 2 (b) Boundary integral equation for the domain point

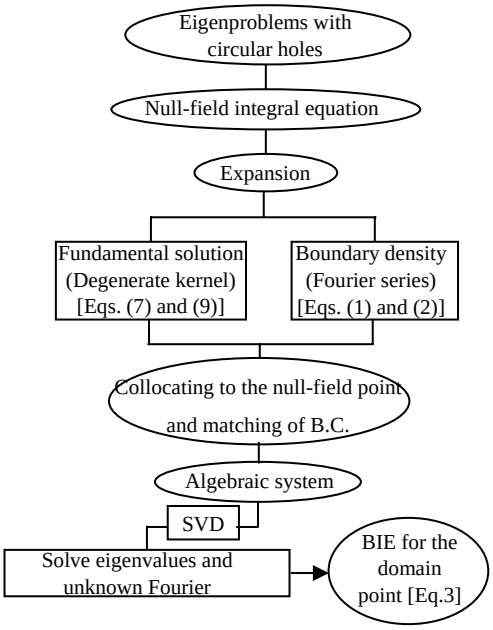

FIGURE 2 (c) The flowchart to determine the eigenvalues and mode shape.

Discussion on Spurious Eigenvalues

For the multiply-connected problem with a circular domain with radius a, Eq. (12) yields

$$\begin{bmatrix} \cdots & J_0(ka)H_0(k\rho) & \cdots & J_M(ka)H_M(k\rho)\cos m\theta_1 & J_M(ka)H_M(k\rho)\sin m\theta_1 & \cdots \\ \cdots & J_0(ka)H_0(k\rho) & \cdots & J_M(ka)H_M(k\rho)\cos m\theta_2 & J_M(ka)H_M(k\rho)\sin m\theta_2 & \cdots \\ \cdots & \vdots & \ddots & \vdots & \vdots & \cdots \\ \cdots & J_0(ka)H_0(k\rho) & \cdots & J_M(ka)H_M(k\rho)\cos m\theta_{2M+1} & J_M(ka)H_M(k\rho)\sin m\theta_{2M+1} & \cdots \\ \cdots & J_0(ka)H_0(ka) & \cdots & J_M(ka)H_M(ka)\cos m\theta_1 & J_M(ka)H_M(ka)\sin m\theta_1 & \cdots \\ \cdots & J_0(ka)H_0(ka) & \cdots & J_M(ka)H_M(ka)\cos m\theta_2 & J_M(ka)H_M(ka)\sin m\theta_2 & \cdots \\ \cdots & \vdots & \ddots & \vdots & \vdots & \cdots \\ \cdots & J_0(ka)H_0(ka) & \cdots & J_M(ka)H_M(ka)\cos m\theta_{2M+1} & J_M(ka)H_M(ka)\sin m\theta_{2M+1} & \cdots \end{bmatrix} \begin{Bmatrix} \vdots \\ p_{0j} \\ \vdots \\ p_{Mj} \\ q_{Mj} \\ \vdots \end{Bmatrix} = \underset{\sim}{0} \quad (13)$$

for the Dirichlet problem. The determinant of the influence matrix is zero for $J_M(ka)=0, \quad M=0,1,2,3\cdots$. This is to say, the eigenvalue for the Dirichlet problem of circular domain with the radius a, is the possible eigenvalue for the considered problem. The possible eigenvalues of $J_M(ka)=0$, are found to be the true eigenvalues of a circular domain with radius a subject to the Dirichlet boundary condition. This finding extends the proof of existence of spurious eigenvalues for annular case [4, 5]. We can claim that any inner circle introduces the spurious eigenvalue for the multiply-connected problems. The spurious eigenvalues are found to be the true eigenvalues of the eigenproblem of inner circle.

Numerical Results and Discussion

In order to demonstrate the validity of the present method, several examples are given.

Example 1. An eccentric case with radii r_1 and r_2 ($r_1=0.5, r_2=2.0$) is shown in Fig. 3(a). The Dirichlet boundary condition is considered. Table 1 shows the former five eigenvalues by using different methods. Good agreement is made. Fig. 3(b) shows the minimum singular value versus *k* where the drop indicates the possible eigenvalues. The present method obtains almost the same result of BEM [2] where a spurious eigenvalue appears at $k=4.81$ ($J_0(4.81r_1)=0$). The spurious eigenvalue was filtered out by using Burton and Miller approach [4]. By adopting the truncated Fourier series (M=10), the mode shapes are shown in Fig.3(c) and compared with those by FEM and BEM are also shown in Fig. 3(d).

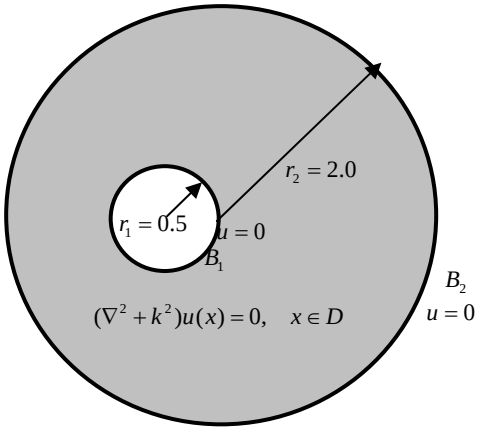

FIGURE 3(a) Eigenproblem with an eccentric domain.

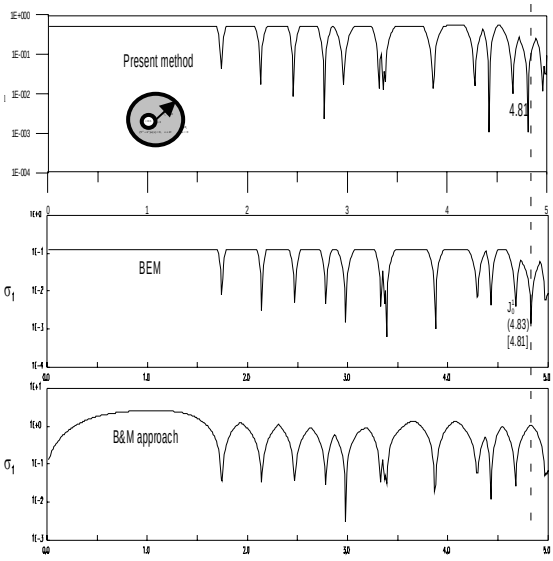

FIGURE 3 (b) The minimim singular σ_1 versus k using different approaches for the Dirichlet problem with an eccentric domain.

TABLE1 The former five eigenvalues of with an eccentric domain.

	1	2	3	4	5
FEM[2]	1.73	2.13	2.45	2.76	2.95
Chen and Zhou[11]	1.75	2.14	2.47	2.78	2.97
BEM[2]	1.74	2.14	2.47	2.78	2.98
Present method	1.74	2.14	2.46	2.78	2.96

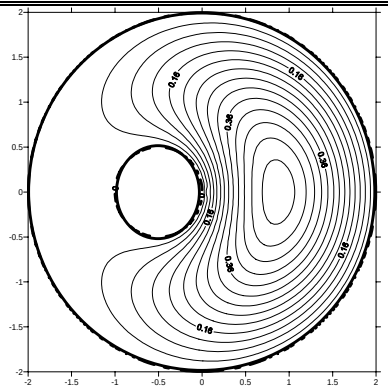

$k = 1.74$

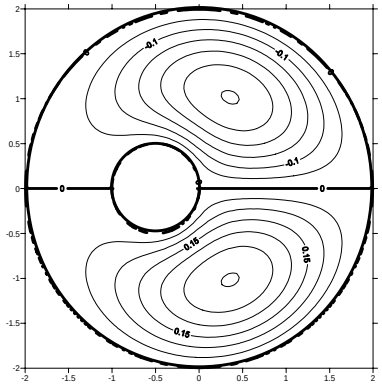

$k = 2.14$

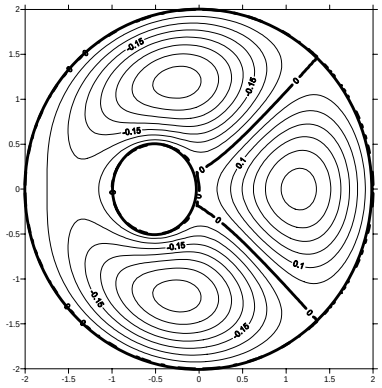

$k = 2.46$

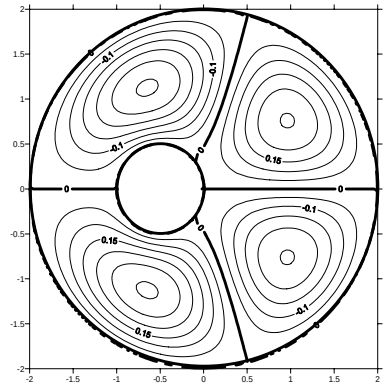

$k = 2.78$

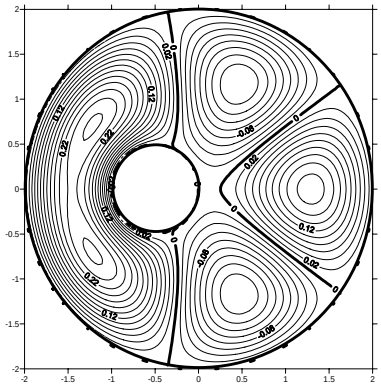

$k = 2.96$

FIGURE 3(c) The former five eigenmodes for an eccentric case using the present method.

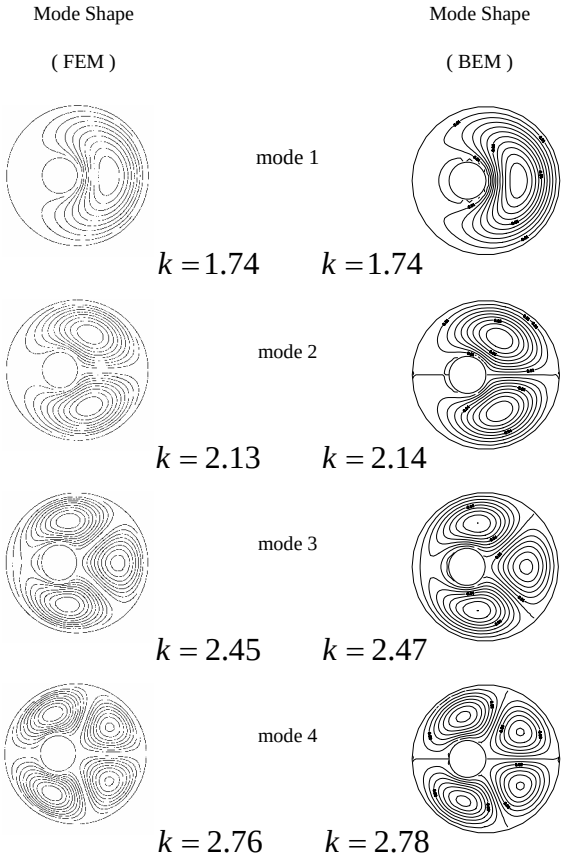

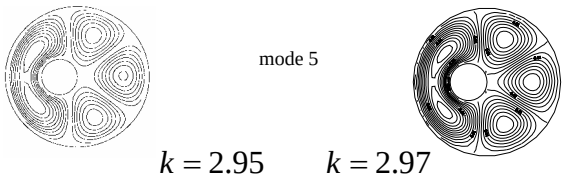

$k = 2.95$　　$k = 2.97$

FIGURE 3(d) The former five eigen-modes for eccentric case using FEM and BEM.

Example 2. A circular region of radius R with two unequal circular holes which are placed on a concentric circle of radius e ($e = 0.5$) as shown in Fig. 4 (a). The radii of the circular holes and the external boundary are $c_1 = 0.3$, $c_2 = 0.4$ and $R = 1.0$. The Dirichlet boundary condition is considered. Table 2 shows the former five eigenvalues by using different methods. Good agreement is made. By adopting truncated Fourier series (M=10), the mode shapes are shown in Fig. 4(b) and are compared with those by BEM and FEM as shown in Fig.4(c).

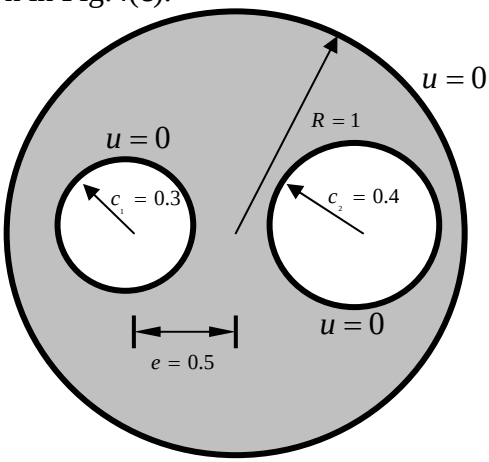

FIGURE 4 (a) Two unequal circular holes in a circular domain

TABLE 2 The former five eigenvalues for a circle domain with two unequal holes

	1	2	3	4	5
FEM[1]	4.79	4.80	6.61	6.63	7.8
BEM[1]	4.82	4.82	6.72	6.72	7.82
Present method	4.85	4.85	6.77	6.77	7.91

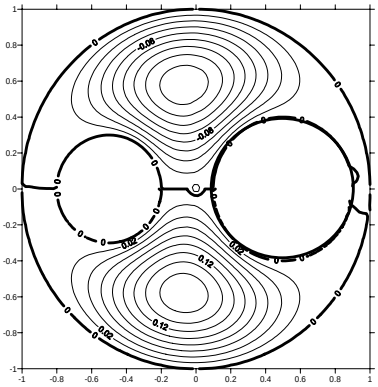

$k = 4.85$

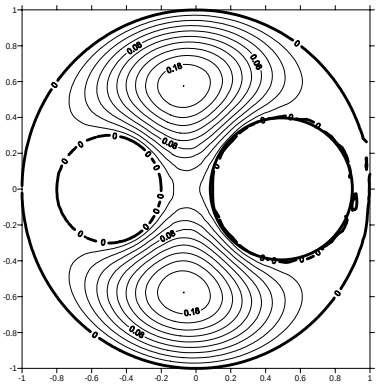

$k = 4.85$

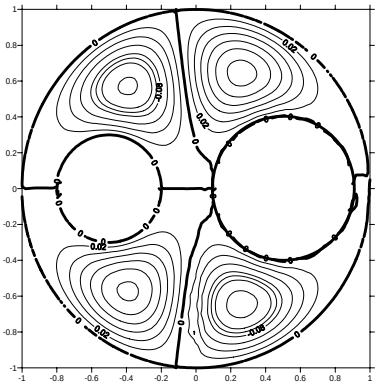

$k = 6.67$

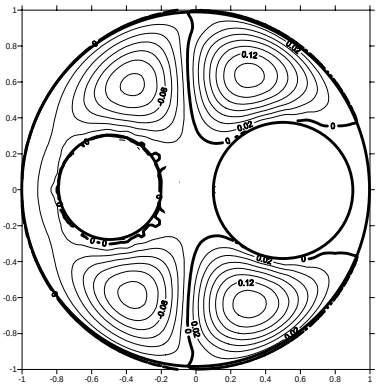

$k = 6.67$

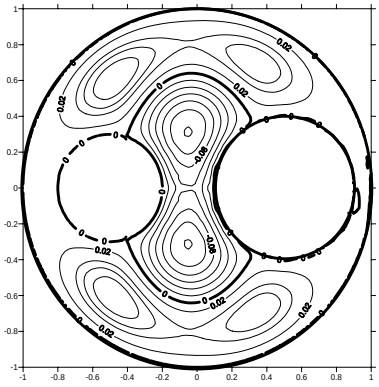

$k = 7.91$

FIGURE 4 (b) The former five modes for a circular domain with two unequal holes by using the present method.

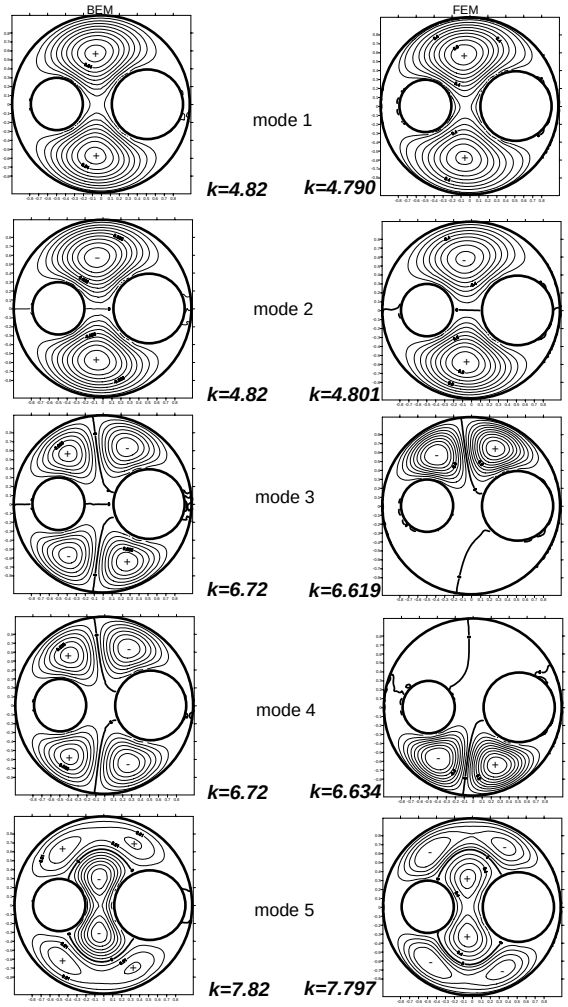

FIGURE 4 (c) The former five modes for a circle domain with two unequal holes using FEM and BEM.

Conclusions

For the eigenproblems with circular boundaries, we have proposed a special BIEM by using degenerate kernels, null-field integral equation and Fourier series in an adaptive observer system. The method shows great generality and versatility for the problems with multiple circular holes of arbitrary radii and positions. Also, the occurrence of spurious eigenvalue was examined. Numerical results agree very well with those of the BEM and FEM.

References

1. Chen, J. T., Liu, L. W., and Chyuan, S. W., "Acoustic Eigenanalysis for Multiply-connected Problems Using Dual BEM," *Communication in Numerical Method in Engineering*, 20, pp. 419-440 (2004).
2. Chen, J. T., Lin, J. H., Kuo, S. R., and Chyuan, S. W., "Boundary Element Analysis for the Helmholtz Eigenvalue Problems with a Multiply Connected Domain," *Proceedings of the Royal Society of London Series A*, 457, pp. 2521-2546 (2001).
3. Chen, J. T., Liu, L. W., and Hong, H-K., "Spurious and True Eigensolutions of Helmholtz BIEs and BEMs for a Multiply Connected Problem," *Proceedings of the Royal Society of London Series A*, 459, pp. 1891-1924 (2003).
4. Chen, J. T., Chen, I. L. and Lee, Y. T., "Eigensolutions of Multiply-Connected Membranes using the Method of Fundamental Solution,"

Engineering Analysis with Boundary Elements, Revised (2004).

5. Lee, Y. T., Chen, I. L, Chen, K. H. and Chen, J. T. "Mathematical Analysis of True and Spurious Eigenvalues for Annular Plates Using the Method of Fundamental Solutions," *The 12th National Conference on Sound and vibration*, Taipei, Taiwan (2004).
6. Lee, Y. T., Chen, J. T. and Chen, I. L., "Free Vibration Analysis of Multiply-connected Plates Using the Method of Fundamental Solutions," *The International Conference on Computational Methods*, Singapore (2004).
7. Lin, W. H., "Guided Waves in a Circular Duct Containing an Assembly of Circular Cylinders," *Journal of Sound and Vibration*, 79, pp. 463-477 (1981).
8. Nagaya, K. and Poltorak, K., "Method for Solving Eigenvalue Problems of the Helmholtz Equation with a Circular Outer and a Number of Eccentric Circular Inner Boundaries," *Journal of the Acoustical Society of America*, 85, pp.576-581 (1989).
9. Chen, G., and Zhou, J., "Boundary Element Methods", *Academic Press* (1992).

二維區域含圓洞之
特徵值問題的新解法

陳佳聰[1] 陳義麟[2] 陳正宗[1]

[1]國立台灣海洋大學河海工程系

[2]國立高雄海洋科技大學造船工程系

摘要

本文以勢能理論為基礎，提出以退化核與傅立葉級數展開搭配零場積分方程求解含多孔洞二維特徵值問題，此方法可視為半解析法。邊界未知勢能與流通量使用有限項傅立葉級數來近似求得。利用退化核與傅立葉展開可導得一線性代數方法而無須對邊界離散。再靠奇異值分解法來求得特徵值及傅立葉係數。文中以幾個不同邊界條件的特徵值問題進行測試。所得結果無論與邊界元素法的數值結果或有限元素法的數值結果比較，均可驗證本方法的正確性。

關鍵字：零場積分方程式，奇異值分解，退化核，傅立葉級數，特徵值問題。

Appendix

(1) For the null-field integral equation of Eq. (6) in Fig. 2 (a), we have ($\left|\underset{\sim}{s}-\underset{\sim}{c}_j\right|>\left|\underset{\sim}{x}-\underset{\sim}{c}_j\right|$).

$$\int_{B_j} U(\underset{\sim}{s},\underset{\sim}{x})t_j(\underset{\sim}{s})dB(\underset{\sim}{s})$$

$$=\int_0^{2\pi}[\frac{-\pi i}{2}\sum_{m=0}^{\infty}\varepsilon_m J_m(k|\underset{\sim}{x}-\underset{\sim}{c}_j|)H_m^{(1)}(k|\underset{\sim}{s}-\underset{\sim}{c}_j|)\cos(m\alpha)]$$

$$[p_{oj}+\sum_{n=1`}^{M}(p_{nj}\cos n\theta+q_{nj}\sin n\theta)]a_j d\theta$$

$$=-\pi^2 i a_j J_0(k|\underset{\sim}{x}-\underset{\sim}{c}_j|)H_0^{(1)}(k|\underset{\sim}{s}-\underset{\sim}{c}_j|)p_{oj}$$

$$-\sum_{m=1}^{M}\{p_{mj}\pi^2 i a_j J_m(k|\underset{\sim}{x}-\underset{\sim}{c}_j|)H_m^{(1)}(k|\underset{\sim}{s}-\underset{\sim}{c}_j|)\cos m\phi$$

$$+q_{mj}\pi^2 i a_j J_m(k|\underset{\sim}{x}-\underset{\sim}{c}_j|)H_m^{(1)}(k|\underset{\sim}{s}-\underset{\sim}{c}_j|)\sin m\phi]\}$$

$$\int_{B_j} T(\underset{\sim}{s},\underset{\sim}{x})u_j(\underset{\sim}{s})dB(\underset{\sim}{s})$$

$$=\int_0^{2\pi}[\frac{-\pi i}{2}\sum_{m=0}^{\infty}\varepsilon_m J_m(k|\underset{\sim}{x}-\underset{\sim}{c}_j|)$$

$$\{\frac{\partial H_m^{(1)}(k|\underset{\sim}{s}-\underset{\sim}{c}|)}{\partial n_s}\cos(m\alpha)+$$

$$H_m^{(1)}(k|\underset{\sim}{s}-\underset{\sim}{c}|)\frac{\partial\cos(m\alpha)}{\partial n_s}\}]$$

$$[a_{oj}+\sum_{n=1`}^{M}(a_{nj}\cos n\theta+b_{nj}\sin n\theta)]a_j d\theta$$

$$=[-\pi^2 i a_{oj}J_0(k|\underset{\sim}{x}-\underset{\sim}{c}_j|)\{\frac{\partial H_0^{(1)}(k|\underset{\sim}{s}-\underset{\sim}{c}|)}{\partial n_s}]$$

$$-\sum_{m=1}^{M}(\pi^2 i a_j a_{mj}J_m(k|\underset{\sim}{x}-\underset{\sim}{c}_j|)\{\frac{\partial H_m^{(1)}(k|\underset{\sim}{s}-\underset{\sim}{c}|)}{\partial n_s}\cos(m\alpha)+$$

$$H_m^{(1)}(k|\underset{\sim}{s}-\underset{\sim}{c}|)\frac{\partial\cos(m\alpha)}{\partial n_s}\})\cos m\phi$$

$$+(\pi^2 i a_j b_{mj}J_m(k|\underset{\sim}{x}-\underset{\sim}{c}_j|)\{\frac{\partial H_m^{(1)}(k|\underset{\sim}{s}-\underset{\sim}{c}|)}{\partial n_s}\cos(m\alpha)+$$

$$H_m^{(1)}(k|\underset{\sim}{s}-\underset{\sim}{c}|)\frac{\partial\cos(m\alpha)}{\partial n_s}\})\sin m\phi]\}$$

where $\left|\underset{\sim}{s}-\underset{\sim}{c}_j\right|=R$, $\left|\underset{\sim}{x}-\underset{\sim}{c}_j\right|=\rho$, θ and ϕ are shown in Fig. 5.

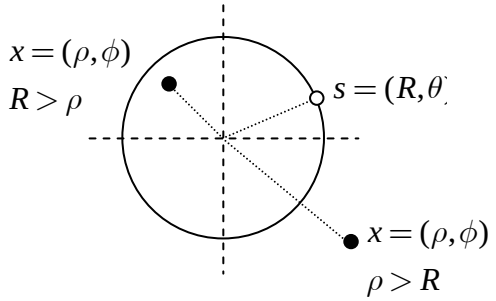

FIGURE 5 Sketch of the source and field points

(2) For the interior point of Eq. (3) in Fig. 2 (b), we have ($\left|\underset{\sim}{x}-\underset{\sim}{c}_j\right|>\left|\underset{\sim}{s}-\underset{\sim}{c}_j\right|$).

$$\int_{B_j} U(\underset{\sim}{s},\underset{\sim}{x})t_j(\underset{\sim}{s})dB(\underset{\sim}{s})$$

$$=\int_0^{2\pi}[\frac{-\pi i}{2}\sum_{m=0}^{\infty}\varepsilon_m H_m^{(1)}(k|\underset{\sim}{x}-\underset{\sim}{c}_j|)J_m(k|\underset{\sim}{s}-\underset{\sim}{c}_j|)\cos(m\alpha)]$$

$$[p_{oj}+\sum_{n=1`}^{M}(p_{nj}\cos n\theta+q_{nj}\sin n\theta)]a_j d\theta$$

$$=-\pi^2 i a_j H_0^{(1)}(k|\underset{\sim}{x}-\underset{\sim}{c}_j|)J_0(k|\underset{\sim}{s}-\underset{\sim}{c}_j|)p_{oj}$$

$$-\sum_{m=1}^{M}\{p_{mj}\pi^2 i a_j H_m^{(1)}(k|\underset{\sim}{x}-\underset{\sim}{c}_j|)J_m(k|\underset{\sim}{s}-\underset{\sim}{c}_j|)\cos m\phi$$

$$+q_{mj}\pi^2 i a_j H_m^{(1)}(k|\underset{\sim}{x}-\underset{\sim}{c}_j|)J_m(k|\underset{\sim}{s}-\underset{\sim}{c}_j|)\sin m\phi]\}$$

$$\int_{B_j} T(\underset{\sim}{s},\underset{\sim}{x})u_j(\underset{\sim}{s})dB(\underset{\sim}{s})$$

$$=\int_0^{2\pi}[\frac{-\pi i}{2}\sum_{m=0}^{\infty}\varepsilon_m H_m^{(1)}(k|\underset{\sim}{x}-\underset{\sim}{c}_j|)$$

$$\{\frac{\partial J_m(k|\underset{\sim}{s}-\underset{\sim}{c}|)}{\partial n_s}\cos(m\alpha)+$$

$$J_m(k|\underset{\sim}{s}-\underset{\sim}{c}|)\frac{\partial\cos(m\alpha)}{\partial n_s}\}]$$

$$[a_{oj}+\sum_{n=1`}^{M}(a_{nj}\cos n\theta+b_{nj}\sin n\theta)]a_j d\theta$$

$$=[-\pi^2 i a_j a_{oj}H_0^{(1)}(k|\underset{\sim}{x}-\underset{\sim}{c}_j|)\{\frac{\partial J_0(k|\underset{\sim}{s}-\underset{\sim}{c}|)}{\partial n_s}]$$

$$-\sum_{m=1}^{M}(\pi^2 i a_j a_{mj}H_m^{(1)}(k|\underset{\sim}{x}-\underset{\sim}{c}_j|)\{\frac{\partial J_m(k|\underset{\sim}{s}-\underset{\sim}{c}|)}{\partial n_s}\cos(m\alpha)+$$

$$H_m^{(1)}(k|\underset{\sim}{s}-\underset{\sim}{c}|)\frac{\partial\cos(m\alpha)}{\partial n_s}\})\cos m\phi$$

$$+(\pi^2 i a_j b_{mj}H_m^{(1)}(k|\underset{\sim}{x}-\underset{\sim}{c}_j|)\{\frac{\partial J_m(k|\underset{\sim}{s}-\underset{\sim}{c}|)}{\partial n_s}\cos(m\alpha)+$$

$$H_m^{(1)}(k|\underset{\sim}{s}-\underset{\sim}{c}|)\frac{\partial\cos(m\alpha)}{\partial n_s}\})\sin m\phi]\}$$